

CONF- 960781--1

SAND96-0619C

## MAGNETIC BREAKDOWN IN DOUBLE QUANTUM WELLS

N. E. HARFF<sup>a,c</sup>, J. A. SIMMONS<sup>a</sup>, G. S. BOEBINGER<sup>b</sup>, J. F. KLEM<sup>a</sup>,  
L. N. PFEIFFER<sup>b</sup>, and K. W. WEST<sup>b</sup>

<sup>a</sup> Sandia National Laboratories, P. O. Box 5800, Albuquerque, NM 87185 USA

<sup>b</sup> Bell Labs, Lucent Technologies, Murray Hill NJ 07974 USA

<sup>c</sup> Oregon State University, Corvallis, OR 97330 USA

### ABSTRACT

We find that a sufficiently large perpendicular magnetic field ( $B_{\perp}$ ) causes magnetic breakdown (MB) in coupled double quantum wells (QWs) that are subject to an in-plane magnetic field ( $B_{\parallel}$ ).  $B_{\parallel}$  shifts one QW dispersion curve with respect to that of the other QW, resulting in an anticrossing and an energy gap. When the gap is below the Fermi level the resulting Fermi surface (FS) consists of two components, a lens-shaped inner orbit and an hour-glass shaped outer orbit.  $B_{\perp}$  causes Landau level formation and Shubnikov-de Haas (SdH) oscillations for each component of the FS. MB occurs when the magnetic forces from  $B_{\perp}$  become dominant and the electrons move on free-electron circular orbits rather than on the lens and hour-glass orbits. MB is observed by identifying the peaks present in the Fourier power spectrum of the longitudinal resistance vs.  $1/B_{\perp}$  at constant  $B_{\parallel}$ , an arrangement achieved with an in-situ tilting sample holder. Results are presented for two strongly coupled GaAs/AlGaAs DQW samples.

The main effect of a magnetic field ( $B_{\parallel}$ ) applied parallel to the growth plane of a DQW is a linear transverse shift of one QW dispersion curve with respect to that of the other QW. The amount of shift is given by  $\Delta k = e d B_{\parallel} / \hbar$  where  $d$  is the distance between the two electron layers. When the coupling between the QWs is strong, the two QW dispersion curves anticross and a partial energy gap ( $E_G$ ) opens,<sup>1</sup> where  $E_G \approx \Delta_{SAS}$ , the symmetric-antisymmetric gap observed in DQWs with equal electron densities at  $B = 0$  T. The partial energy gap can be moved upward in energy by increasing  $B_{\parallel}$ . Features are observed in the in-plane conductance as the energy gap is moved through the Fermi energy ( $E_F$ ).<sup>2</sup> At low  $B_{\parallel}$ , when the energy gap is below  $E_F$ , the resulting Fermi surface (FS) has two components; an inner lens-shaped orbit and an outer hour-glass-shaped one. This FS is shown in the inset of Fig. 1(a) for a DQW with unequal electron densities. A perpendicular magnetic field ( $B_{\perp}$ ) causes Landau level formation and Shubnikov-de Haas (SdH) oscillations for each branch of the FS. At higher  $B_{\perp}$ , magnetic breakdown occurs when  $B_{\perp}$  causes electrons to tunnel across the gap in  $\mathbf{k}$ -space from one FS branch to another.<sup>3,4</sup>

Here we report magnetotransport measurements on DQWs subject to constant  $B_{\parallel}$  and changing  $B_{\perp}$ .  $B_{\parallel}$  defines the FS and  $B_{\perp}$  allows its characterization through the SdH

## **DISCLAIMER**

**Portions of this document may be illegible  
in electronic image products. Images are  
produced from the best available original  
document.**

TABLE I. Sample parameters.

Sample	$w / t$ (Å)	$n$ ( $10^{11} \text{ cm}^{-2}$ )		$\mu$ ( $10^3 \text{ cm}^2/\text{Vs}$ )	$\Delta_{\text{SAS}}$ (meV)
		$n_{\text{top}}$	$n_{\text{bottom}}$		
A	150 / 15	1.9	1.1	310	2.3
B	139 / 28	2.1	2.4	740	1.5

oscillations. In this way the areas of the different components of the FS can be extracted. At higher values of  $B_{\perp}$ , magnetic breakdown is seen to occur for a wide range of  $B_{\parallel}$ .

We measured two samples that consisted of symmetric modulation-doped GaAs QWs of width  $w$  separated by an  $\text{Al}_{0.3}\text{Ga}_{0.7}\text{As}$  barrier of thickness  $t$ . Table I lists the values of  $w$  and  $t$  along with the densities ( $n_{\text{top}}$  and  $n_{\text{bottom}}$ ) in each QW, the sample mobility, and  $\Delta_{\text{SAS}}$ . Sample A is a 0.2 mm wide Hall bar and Sample B is a Van der Pauw square 3 mm on a side. Standard four-terminal lock-in measurements were performed at  $T = 0.3$  K. To achieve constant  $B_{\parallel}$  with changing  $B_{\perp}$  in a total magnetic field  $B_{\text{T}}$ , a series of several hundred  $B_{\text{T}}$ -sweeps is done with the sample mounted at different angles  $\theta$  from perpendicular with *in situ* rotation possible. A schematic of the sample and the magnetic field components are shown in the inset to Fig 1(c). The angle is held constant during a sweep and changed between sweeps at a rate sufficiently slow that the sample temperature remains below 1 K.  $\theta$  is determined using two Hall probes; one measures  $B_{\text{T}}$ , while the other is mounted on the tilting stage to measure  $B_{\perp}$  only. After the scans are finished, a trace of  $R_{xx}$  as a function of  $B_{\perp}$  at constant  $B_{\parallel}$  is then extracted from the data.

Three such traces are shown in Fig. 1. The magnetoresistance shows SdH oscillations with beating due to multiple orbits taking part in the transport. The orbits producing the SdH oscillations can be identified using the fact that the frequency of oscillation in  $1/B_{\perp}$  is proportional to the orbit's area in  $\mathbf{k}$ -space. At low  $B_{\perp}$ , the Sample A trace for  $B_{\parallel} = 5.0$  T (Fig. 1(a)) shows single-period low frequency oscillations from the lens orbit. At intermediate  $B_{\perp}$ , higher frequency oscillations from the hour-glass orbit are superimposed on these oscillations, while at higher  $B_{\perp}$ ,

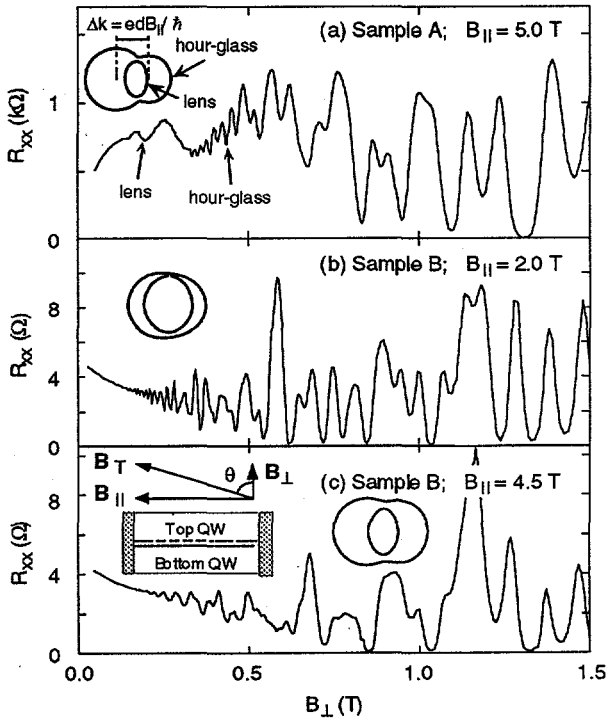


Fig. 1. Magnetoresistance as a function of  $B_{\perp}$ . The insets show the corresponding Fermi surfaces and a schematic drawing of the sample showing the QWs and the orientation of the magnetic field.

the frequency components in the oscillations are more difficult to identify visually. In Fig. 1(b) and (c), the frequency components are difficult to identify visually at all  $B_{\parallel}$ .

To identify the frequency components present, the Fourier power spectrum of  $R_{xx}$  as a function of  $1/B_{\perp}$  is computed using a fast Fourier Transform (FFT) algorithm with  $B_{\perp}$  in the range 0.1 – 1.2 T. Fig. 2 shows the Fourier power spectra for the three scans in Fig. 1. In all three data sets we can identify several peaks corresponding to different FS orbits: a low frequency peak from the lens orbit, a high frequency peak from the hour-glass orbit, and two intermediate frequency peaks from the QW circle orbits. The presence of the circle orbits indicates that magnetic breakdown is occurring because the

electrons must tunnel across the gap in  $\mathbf{k}$ -space to traverse the circle orbits. The probability of tunneling is given by  $P = \exp(-B_{\perp}^0/B_{\perp})$  where  $B_{\perp}^0$  is the breakdown field.<sup>3,4</sup>

An experimental determination of  $B_{\perp}^0$  is desired for comparison with theory, however,  $B_{\perp}^0$  is difficult to quantify in this experiment. When  $B_{\perp} = B_{\perp}^0$ , significant MB is occurring and the circle orbits are making major contributions to the SdH oscillations. However, this point is difficult to identify in the data for two reasons. First, a visual determination of  $B_{\perp}^0$  from the  $R_{xx}$  data is not possible because the circle orbit oscillations cannot be identified by the naked eye. Second, a determination of  $B_{\perp}^0$  might be made by measuring the Fourier power over small windows of  $B_{\perp}$ , shifting the center of the window to increasingly higher  $B_{\perp}$  values for each spectrum. We were unable to use this method reliably because the resolution of the Fourier spectrum was greatly reduced with small  $B_{\perp}$  windows, which included only a couple of oscillations from each orbit. However, a rough estimate of  $B_{\perp}^0$  is possible for Sample A at  $B_{\parallel} = 5.0$  T. In Fig. 1(a) at low  $B_{\perp}$ , only a single frequency oscillation is present below  $B_{\perp} \approx 0.3$  T, indicating MB has not yet occurred, while from Fig. 2(a), we see that MB is occurring before  $B_{\perp} = 1.2$  T, the upper limit of the FFT. Thus  $B_{\perp}^0$  is in the range  $\approx 0.3 – 1.2$  T. This gives order of magnitude agreement with Hu et. al.'s results<sup>2</sup> which predict  $B_{\perp}^0 = 0.5$  T for this sample. However, a more precise determination of  $B_{\perp}^0$  is needed for meaningful comparison with theory.

The Fourier frequencies of the various orbits of Sample B are shown in Fig. 3 as a function of  $B_{\parallel}$ . As expected, the size of the lens orbit decreases and size of the hour-glass orbit increases with increasing  $B_{\parallel}$ , while the two QW circle orbits are relatively unaffected

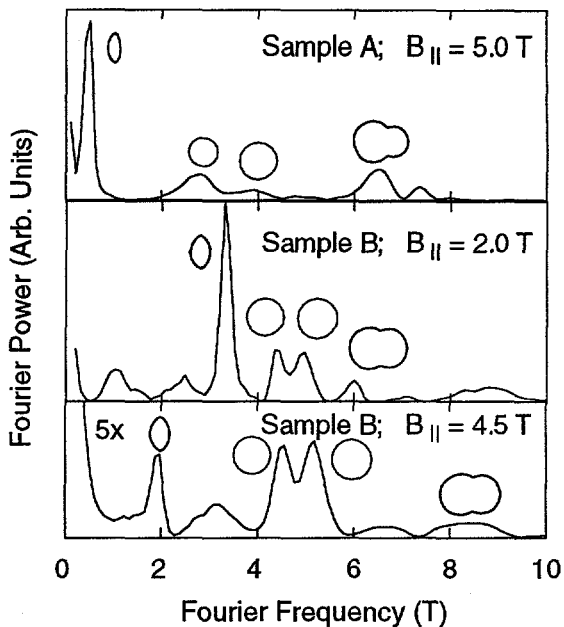


Fig. 2. Fourier power spectrum of  $R_{xx}$  vs.  $1/B_{\perp}$  for the traces of Fig. 1. The peaks are labeled with sketches of their corresponding orbits. The presence of the circle orbits indicates that magnetic breakdown is occurring.

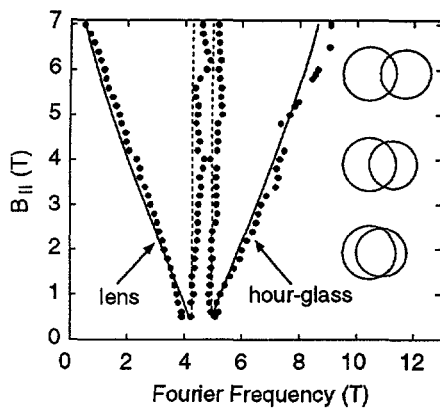


Fig. 3. Plot of the Fourier frequencies of the FS orbits vs.  $B_{\parallel}$  for Sample B. The symbols are the measured frequencies. The dashed lines are the measured  $B_{\parallel} = 0$  T circle orbit frequencies and the solid lines are the geometrically calculated frequencies for the lens and hour-glass orbits. Sketches of the Fermi surfaces for distortion of the single QW FS by  $B_{\parallel}$  which gives the FS an 'egg-like' shape at high  $B_{\parallel}$  and increases the orbit's area.<sup>5</sup>

In conclusion, we present magnetotransport data for strongly coupled DQWs subject to a constant in-plane magnetic field with a changing component of perpendicular field. The in-plane field shifts one QW dispersion curve with respect to that of the other QW resulting in an anticrossing of the two curves which yields a FS that consists of two components. Magnetic breakdown occurs when  $B_{\perp}$  causes electrons to tunnel across the gap in  $\mathbf{k}$ -space from one FS branch to another. The magnetoresistance exhibits beating due to a FS that consists of several closed orbits that are the result of  $B_{\parallel}$ -induced distortions of the FS as well as  $B_{\perp}$ -induced distortions due to magnetic breakdown. Magnetic breakdown is observed by noting which peaks are present in the Fourier power spectrum of the magnetoresistance versus  $1/B_{\perp}$ . We observe magnetic breakdown over a range of  $B_{\parallel}$  in both DQW samples studied. Further experiments are in progress to better quantify the magnetic breakdown field  $B_{\perp}^0$  for comparison with theory.

Acknowledgment—This work was supported by the U.S. Department of Energy under Contract DE-AC04-94AL85000.

## References

1. S. K. Lyo, *Phys. Rev. B* **50**, 4965 (1994).
2. J. A. Simmons, S. K. Lyo, N. E. Harff, and J. F. Klem, *Phys. Rev. Lett.* **73**, 2256 (1994).
3. E. I. Blount, *Phys. Rev.* **126**, 1536 (1962).
4. J. Hu and A. H. MacDonald, *Phys. Rev. B* **46**, 12 554 (1992).
5. L. Smrcka and T. Jungwirth, *J. Phys.: Condens. Matter* **6**, 55 (1994).

by  $B_{\parallel}$ . The circle orbits indicate that MB is occurring over a wide range of  $B_{\parallel}$ . Also shown are the measured  $B_{\parallel} = 0$  T circle orbit frequencies and the geometrically predicted frequencies for the lens and hour-glass orbits. The areas of these orbits are calculated from the area of the two  $B_{\parallel} = 0$  T QW circle orbits and the relative shift between them, and then converted to frequency. The agreement between the experimental and calculated frequencies is quite good. The effect of the energy gap is ignored in these calculations. Although including this effect would result in a decrease in the lens orbit frequencies and an increase in the hour-glass orbit frequencies, the changes would be very small for this sample because  $\Delta_{\text{SAS}}$  is relatively small. We note that the measured circle orbit frequencies increase slightly with increasing  $B_{\parallel}$  due to a slight distortion of the single QW FS by  $B_{\parallel}$  which gives the FS an 'egg-like' shape at high  $B_{\parallel}$  and increases the orbit's area.<sup>5</sup>

## **DISCLAIMER**

This report was prepared as an account of work sponsored by an agency of the United States Government. Neither the United States Government nor any agency thereof, nor any of their employees, makes any warranty, express or implied, or assumes any legal liability or responsibility for the accuracy, completeness, or usefulness of any information, apparatus, product, or process disclosed, or represents that its use would not infringe privately owned rights. Reference herein to any specific commercial product, process, or service by trade name, trademark, manufacturer, or otherwise does not necessarily constitute or imply its endorsement, recommendation, or favoring by the United States Government or any agency thereof. The views and opinions of authors expressed herein do not necessarily state or reflect those of the United States Government or any agency thereof.